Purdue University
Purdue e-Pubs

International Refrigeration and Air Conditioning Conference

School of Mechanical Engineering

2012

Thermodynamic Design of Condensers and Evaporators: Thermodynamic Design of Condensers and Evaporators: Formulation and Applications

Christian Hermes
chermes@ufpr.br

Thermodynamic Design of Condensers and Evaporators: Formulation and Applications

Christian J. L. HERMES

Center for Applied Thermodynamics, Department of Mechanical Engineering, Federal University of Paraná
P.O. Box 19011, 81531990 Curitiba-PR, Brazil, chermes@ufpr.br

ABSTRACT

This paper assesses the approach introduced in a prior publication for the optimum design of condensers and evaporators aimed at balancing the heat transfer and pressure drop tradeoffs. Case studies carried out with different heat exchanger configurations for light commercial and household refrigeration applications are reported. The analysis indicated that a heat exchanger design with a high aspect ratio is preferable to a low aspect ratio one as the former produces a dramatically lower amount of entropy. In addition, since the refrigeration system COP obeys the $T_e/(T_c-T_e)$ scale, it was found that the heat exchanger design that presents the best local (component-level) performance in terms of minimum entropy generation also leads to the best global (system-level) performance.

1. INTRODUCTION

Condensers and evaporators are heat exchangers with fairly uniform wall temperature employed in a wide range of HVAC-R products, spanning from household to industrial applications. In general, they are designed aiming at accomplishing a heat transfer duty at the penalty of pumping power. There are two well-established methods available for the thermal heat exchanger design, the log-mean temperature difference (LMTD) and the effectiveness/number of transfer units (ε-Ntu) approach (Kakaç and Liu, 2002; Shah and Sekulic, 2003). The second has been preferred to the former as the effectiveness, defined as the ratio between the actual heat transfer rate and the maximum amount that can be transferred, provides a 1st-law criterion to rank the heat exchanger performance, whereas the number of transfer units compares the thermal size of the heat exchanger with its capacity of heating or cooling material. Furthermore, the ε-Ntu approach avoids the cumbersome iterative solution required by the LMTD for outlet temperature calculations.

Nonetheless, neither ε-Ntu or LMTD approaches can address the heat transfer / pumping power tradeoffs, which is the crux of a balanced heat exchanger design. For this purpose, Bejan (1987) established the *thermodynamic design* method, later renamed as *entropy generation minimization* method (Bejan, 1996), which balances the thermodynamic irreversibilities associated with heat transfer with a finite temperature difference and with viscous fluid flow, thus providing a 2nd-law criterion that has been widely used for the sake of heat exchanger design and optimization (San and Jan, 2000; Lerou et al., 2005; Saechan and Wongwises, 2008; Mishra et al., 2009; Pussoli et al., 2010; Kotcioglu et al., 2010; Hermes et al., 2012). The models proposed in the studies just mentioned above, however, require complex numerical solutions, being therefore not suitable for HVAC-R engineers in the industrial environment, which have been challenged with more stringent cost and energy targets every year.

In a recent publication, Hermes (2012) put forward an explicit, algebraic formulation which expresses the dimensionless rate of entropy generation as a function of the number of transfer units, the thermal-hydraulic characteristics (j and f curves), and the operating conditions (heat transfer duty, core velocity, coil surface temperature, and fluid properties) for heat exchangers with uniform wall temperature. An expression for the optimum heat exchanger effectiveness, based on the working conditions, heat exchanger geometry and fluid properties, was also presented. The theoretical analysis led to the conclusion that there does exist a number of transfer units and, consequently, a heat exchanger effectiveness which minimize the overall entropy generation in case of diabatic viscous fluid flow.

The present paper is aimed at assessing the formulation introduced by Hermes (2012) for designing condensers and evaporators for refrigeration systems spanning from household ($Q\sim10^2$ W, $\Delta p\sim10$ Pa) to light commercial ($Q\sim10^3$ W, $\Delta p\sim10^2$ Pa) applications, which amounts 10% of the electrical energy consumed worldwide (Melo and Silva, 2010).

2. ALGEBRAIC MODEL

In general, condensers and evaporators for refrigeration applications are designed considering the coil flooded with two-phase refrigerant, and also a wall temperature close to the refrigerant temperature (Barbosa and Hermes, 2012), so that the temperature profiles along the streams are those represented in Fig. 1. In these cases, the heat transfer rate if calculated from:

$$Q = mc_p(T_o - T_i) = \varepsilon mc_p(T_s - T_i) \tag{1}$$

where m is the mass flow rate, T_i, T_o and T_s are the inlet, outlet and surface temperatures, respectively, $Q=hA_s(T_s-T_m)$ is the heat transfer rate, T_m is the mean flow temperature over the heat transfer area, A_s, and ε is the heat exchanger effectiveness, calculated from (Kays and London, 1984):

$$\varepsilon = 1 - \exp(-Ntu) \tag{2}$$

where $Ntu=hA_s/mc_p$ is the number of transfer units. The pressure drop, on the other hand, is calculated from (Kays and London, 1984):

$$\Delta p = p_i - p_o = f\frac{\rho u_c^2}{2}\frac{A_s}{A_c} \tag{3}$$

where f is the friction factor, u_c is the velocity in the minimum flow passage, A_c, and the subscripts "i" and "o" refer to the heat exchanger inlet and outlet ports, respectively. One should note that eqs. (1) and (3) are linked each other through the following Gibbs relation:

$$T_m(s_o - s_i) = c_p(T_o - T_i) - \frac{(p_o - p_i)}{\rho} \tag{4}$$

where the entropy variation, s_o-s_i, is calculated from the 2nd-law of Thermodynamics,

$$s_o - s_i = \frac{1}{m}\left(\frac{Q}{T_s} + S_g\right) \tag{5}$$

where the first term in the right-hand side accounts for the reversible entropy transport with heat (Q/T_s), whereas S_g is the irreversible entropy generation due to both heat transfer with finite temperature difference and viscous flow.

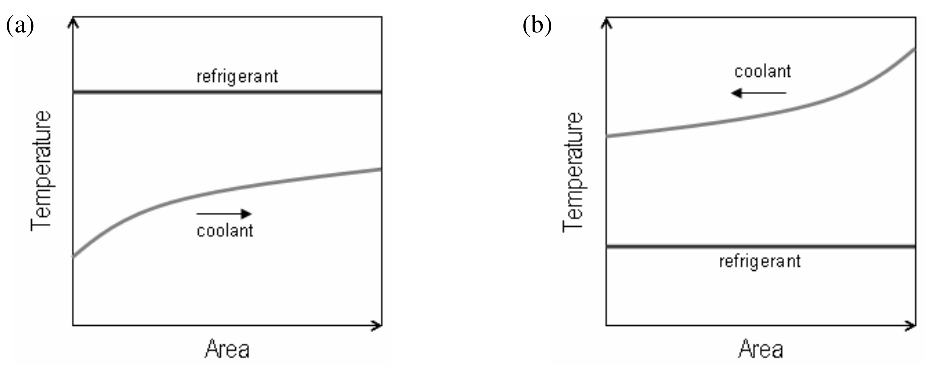

Figure 1: Schematic representation of the temperature profiles in (a) condensers and (b) evaporators

Substituting eqs. (1), (3) and (5) into eq. (4), it follows that:

$$N_S = \frac{S_g}{mc_p} = \frac{Q}{mc_p}\left(\frac{T_s - T_m}{T_s T_m}\right) + \frac{f}{2}\frac{u_c^2}{c_p T_m}\frac{A_s}{A_c} \tag{6}$$

where N_S is the dimensionless rate of entropy generation. Noting that both condensers and evaporators are designed to provide a heat transfer duty subjected to air flow rate and face area constraints, and also that $T_sT_m \approx T_s^2$ and $A_s/A_c = NtuPr^{2/3}/j$, where $j = hPr^{2/3}/\rho c_p u_c$ is the Colburn j-factor, eq. (6) can be re-written as follows (Hermes, 2012):

$$N_S = \Theta^2 Ntu^{-1} + \frac{f}{2j} U^2 Pr^{2/3} Ntu \tag{7}$$

where $U = u_c(c_pT_m)^{-1/2}$ is a dimensionless core velocity, and $\Theta = (T_o - T_i)/T_s$ a dimensionless temperature with both T_o and T_i known from the application. One should note that the first and second terms of the right-hand side of eq. (7) stand for the dimensionless entropy generation rates associated with the heat transfer with finite temperature difference and viscous flow, respectively. The optimum heat exchanger design Ntu^* that minimizes the rate of entropy generation is obtained from (Hermes, 2012):

$$\frac{\partial N_S}{\partial Ntu} = 0 \Rightarrow Ntu^* = \frac{\Theta}{U Pr^{1/3}}\sqrt{\frac{2j}{f}} \tag{8}$$

Eq. (8) shows that there does exist an optimum heat exchanger design (Ntu^*) which leads the overall rate of entropy generation towards a minimum. Basically, it depends on the working conditions (Θ, U), the heat exchanger characteristics (j, f), and the fluid properties (Pr). Since one stream is changing phase, the effectiveness depends only on the number of transfer units (see eq. 2), thus there is also a $0<\varepsilon^*<1$ that minimizes N_S.

One should note that in case where $N_{S,\Delta T} >> N_{S,\Delta p}$ (i.e., high Θ and low U), N_S is minimized either when $\varepsilon \to 1$ (as observed by Bejan (1987) for frictionless fluid flow) or when $\varepsilon \to 0$ (as in the $Ntu \to 0$ limit the heat exchanger vanishes as an engineering component). Additionally, in case where $N_{S,\Delta p} >> N_{S,\Delta T}$ (i.e. high U and low Θ), there is not an optimum as N_S increases steadily with Ntu. The novelty of the eq. (7) relies on the fact that in case where $N_{S,\Delta T} \sim N_{S,\Delta p}$, there does exist a finite Ntu (and also $0<\varepsilon<1$) which drives N_S towards a minimum (Hermes, 2012).

Moreover, an additional assumption comes up from the Chilton-Colburn boundary layer analogy, which states that f=2j for laminar flows over horizontal flat surfaces, suggesting that $f/2j \approx$ constant seems to be a good approximation for a wide range of applications. Figure 2 illustrates eq. (7) with f=2j, $\Theta=0.01$, U=0.01 for various Pr. It can be seen, for Pr=1 (Fig. 2.a), that the dotted lines that cross each other represent the individual contributions of ΔT and Δp to the global rate of entropy generation, which is indicated by the solid line. The dashed line represents the ε-values observed for various Ntu, where it can be noted that $Ntu^* \approx 1$ and $\varepsilon^* \approx 0.63$, since higher Ntu-values (and so ε) increase $N_{S,\Delta p}$, whereas lower Ntu-values increase $N_{S,\Delta T}$, indicating that a high effectiveness heat exchanger has not necessarily the best thermal-hydraulic design, as observed by Hermes (2012).

In addition, it can be noted that the minima move towards lower Ntu for high Pr values (see Fig. 2.b) as Pr>>1 is associated with high momentum diffusivity (high pumping power), so that the irreversibilities due to viscous pressure drop become dominant for relatively low heat exchanger sizes, whereas Pr<<1 (see Fig. 2.c) implies on low heat transfer coefficients, so that the irreversibilities due to heat transfer with finite temperature difference rule. Also, it should be noted that the optimum heat exchanger design is (ε^*, Ntu^*)=(0.88, 2.1) for Pr=0.1, and (ε^*, Ntu^*)=(0.36, 0.44) for Pr=10.

3. CASE STUDIES

For the sake of heat exchanger design, eq. (8) has to be solved concurrently with $\varepsilon = (T_o - T_i)/(T_s - T_i)$ as the coil surface temperature, T_s, must be free to vary thus ensuring that Θ (and so Q and m) is constrained. However, the solution is implicit for T_s, thus requiring an iterative calculation procedure: a guessed T_s value is needed to calculate the effectiveness ε and Ntu=–ln(1–ε), which is used in eq. (8) with j=j(Re) and f=f(Re) curves, and also with the dimensionless core velocity to come out with Θ, which in turn is used to recalculate T_s until convergence is achieved.

(a)

(b)

(c)

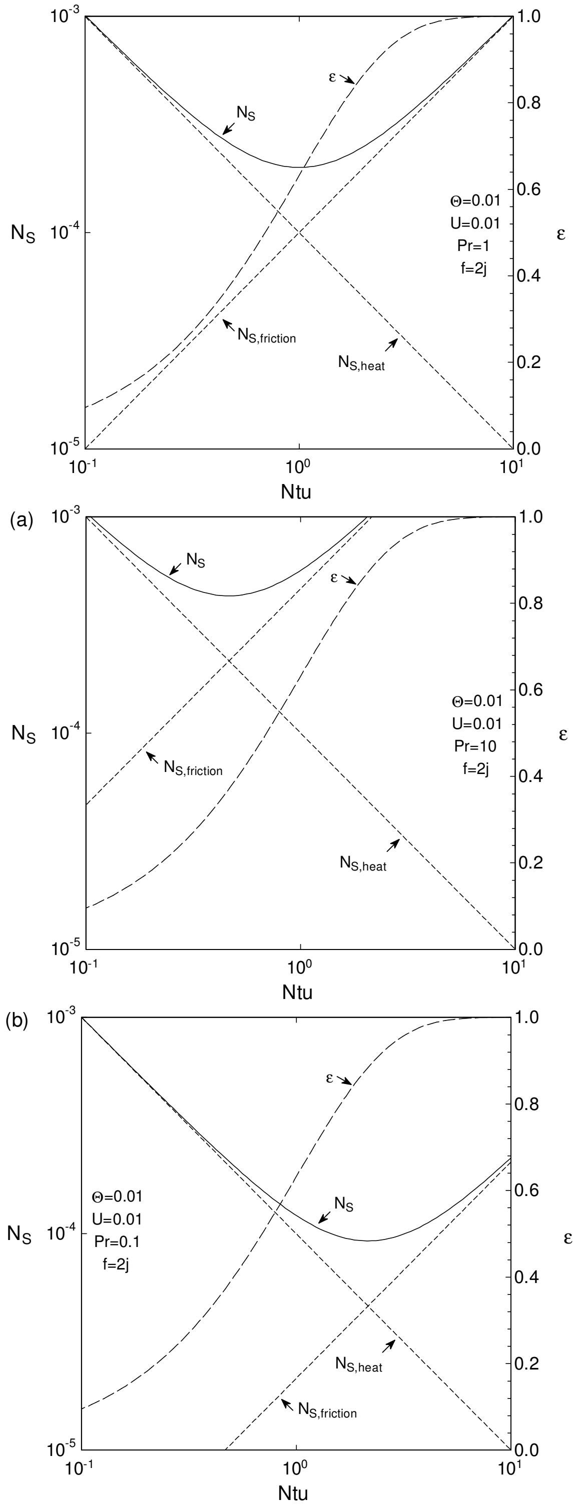

Figure 2: Effect of Ntu on N_S for various Pr (U=0.01, Θ=0.01, f=2j): (a) Pr=1, (b) Pr=10 and (c) Pr=0.1

Consider an air-supplied tube-fin condenser for small-capacity refrigeration appliances running under the following working conditions: Q=1 kW, V=1000 m^3/h, T_i=300K (Hermes et al., 2012). Assume two heat exchanger configurations: (i) circular tubes with flat fins (i.e., Kays and London's surface 8.0-3/8T), whose thermal-hydraulic characteristics are $j=0.16Re^{-0.4}$, $f=0.12Re^{-0.2}$, $\sigma=0.534$ and D_h=3.632 mm, and (ii) circular tubes and fins (Kays and London's surface CF-8.72), whose thermal-hydraulic characteristics are $j=0.22Re^{-0.4}$, $f=0.20Re^{-0.2}$, $\sigma=0.524$ and D_h=3.929 mm. Also note that $Pr\approx0.7$ for air. Figure 3 compares the performance characteristics (j and f curves) of surfaces 8.0-3/8T and CF-8.72 as functions of $Re=\rho u_c D_h/\mu$.

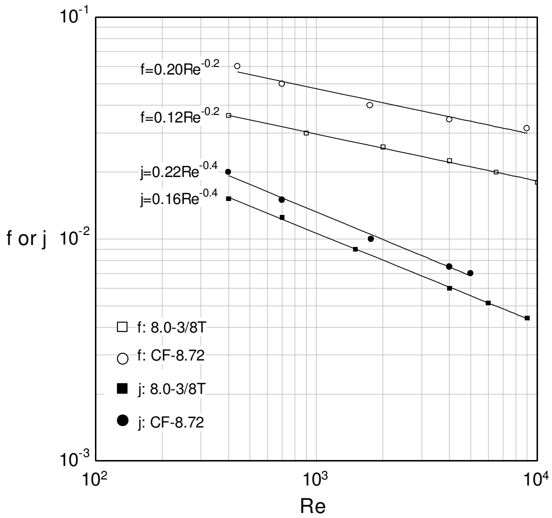

Figure 3: Performance characteristics of surfaces 8.0-3/8T and CF-8.72 (Kays and London, 1984)

Figure 4 compares the dimensionless entropy generation observed for both surfaces as a function of Ntu. A curve of $\varepsilon=\varepsilon(Ntu)$, which is identical for both surfaces, is also plotted to be used as reference. It can be clearly seen that the (ε, Ntu) design which minimizes the rate of entropy generation is (0.61, 0.95) for surface 8.0-3/8T and (0.57, 0.81) for surface CF-8.72. It can also be noted that the circular-fin surface showed a higher rate of entropy generation for all Ntu span, which is mostly due to viscous fluid flow effects as surface CF-8.72 has a higher friction factor than surface 8.0-3/8T for the same Reynolds number (see Fig. 3). For low Ntu values, when the entropy generation is ruled by $N_{S,\Delta T}$, both surfaces showed similar N_S values as their j-curves are close (see Fig. 3).

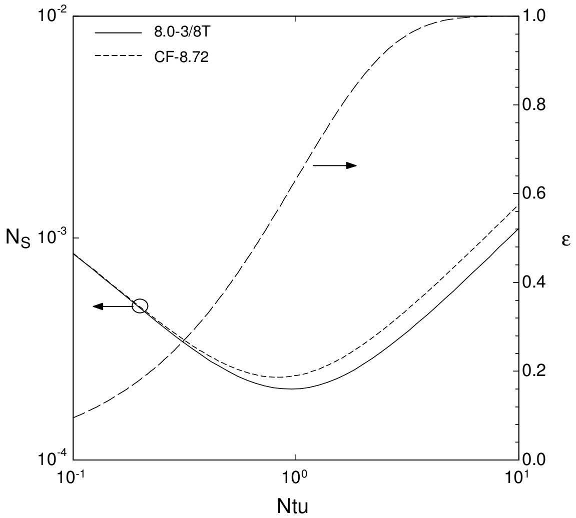

Figure 4: Effect of Ntu on N_S for different condenser configurations (Q=1 kW, V=1000 m^3/h, T_i=300K, A_f=0.1 m^2)

Figure 5 compares three different condenser designs considering surface 8.0-3/8T and face areas varying from 0.025 to 0.1 m^2 under the same working conditions. The heat exchanger length was also varied in order to accommodate the heat transfer surface area for different face areas. For a vertical, constant Ntu line (i.e. same heat transfer area), it can be clearly observed that a heat exchanger design with high aspect ratio (higher face area, smaller length in the flow direction) produces a significantly lower amount of entropy in comparison to a low aspect ratio design (lower face area, larger length). It can be additionally observed that the N_S curves converge for low Ntu values, as the pressure drop effects, which rule the entropy generation for low aspect ratio designs, are attenuated for low Ntu values where the entropy generation is governed by heat transfer with finite temperature difference.

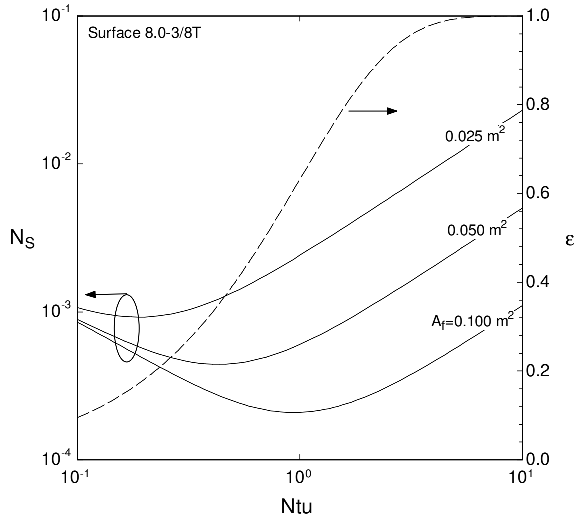

Figure 5: Effect of Ntu on N_S for different condenser face areas (Q=1 kW, V=1000 m^3/h, T_i=300K)

Consider now an air-supplied evaporator for household refrigeration applications, comprised of 10 tube rows in the flow direction and 2 rows in the transversal direction, and whose performance characteristics are as follows (Barbosa et al., 2009): $j \approx 0.69 Re_{Dt}^{-0.48} \phi^{-0.34}$ and $f \approx 2.9 Re_{Dt}^{-0.30} \phi^{-0.77}$, where $\phi \approx 5.8$ is the finning factor, $D_t \approx 8$ mm is the tube O.D., $A_f \approx 0.02$ m^2 and $\sigma \approx 0.72$. The working conditions are: $Q \approx 100$ W, $V \approx 50$ m^3/h, and $T_i \approx 260$K. In the following analysis, the mass transfer and the related frost accretion phenomena were not modeled.

Figure 6 shows the rate of entropy generation as a function of Ntu for the no-frost evaporator. It can be clearly seen that the minimum entropy generation takes place for Ntu~6.5 and $\varepsilon \rightarrow 1$, thus indicating that, in this type of evaporator, the pressure drop effects are not as important as the heat transfer with finite temperature difference. Nonetheless, these figures may change dramatically in case of frost accretion over the evaporator coil, which increases not only the pressure drop but also the thermal conduction resistance.

Figure 7 shows the optimum Ntu diminishes as $\sigma = A_c/A_f$ is reduced (which is likely to occur when frost is formed over the heat exchanger surface), so that $Ntu^*=2$ in case of $\sigma=0.3$. This is so as a higher free flow passage area A_c (i.e. a higher σ for a fixed face area A_f) yields a lower core velocity, u_c, thus requiring an improved heat transfer surface A_s (i.e. a higher Ntu) to accomplish the constrained heat transfer duty. It should be also noted that the minimum dimensionless entropy generation rate increases as σ decreases, indicating that the pressure drop effects become dominant for lower Ntu values. It can also be noted that the curves for different σ converge for low Ntu values, as σ has more influence upon the pressure drop rather than the temperature difference, being the former attenuated for low Ntu values.

4. FINAL REMARKS

This study explored an analytical formulation proposed elsewhere (Hermes, 2012) that conflates two different heat exchanger design methodologies, the Kays and London's (1984) ε-Ntu approach and the Bejan's (1987, 1996) method of entropy generation minimization. It was shown that there does exist a particular ε-Ntu design for condensers and evaporators that minimizes the dimensionless rate of entropy generation. To this observation follows the conclusion that a high effectiveness heat exchanger has not necessarily the best thermal-hydraulic design, as the effectiveness does not account for the pumping power effect.

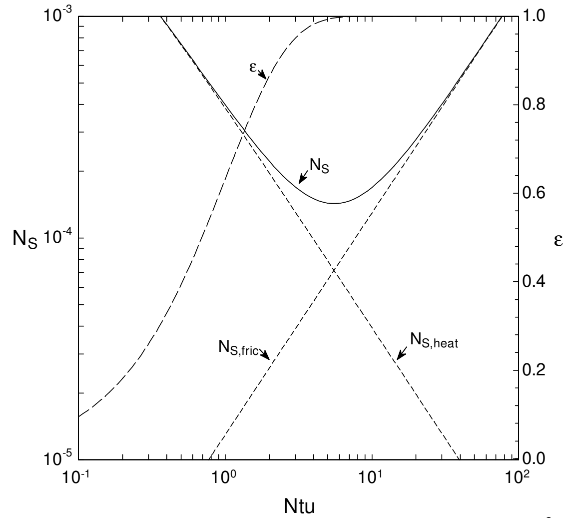

Figure 6: Effect of Ntu on N_S for a no-frost evaporator (Q=100 W, V=50 m^3/h, T_i=260K, A_f=0.02 m^2)

Case studies considering a tube-fin condenser for light commercial refrigeration applications and an evaporator for frost-free refrigerators were also carried out. In case of the condenser coil, where the entropy production due to viscous fluid flow is of the same order of that due to finite temperature difference, the analytical formulation of Hermes (2012) showed to be suitable for thermodynamic optimizations. The analysis also indicated that a heat exchanger design with a high aspect ratio is preferable to a low aspect ratio one as the former produces a dramatically lower amount of entropy. In addition, it was found that in case of a "no-frost" evaporator working under dry coil conditions, the pressure drop influence on the dimensionless entropy production is negligible in comparison to the finite temperature difference, so that eq. (7) should be used with great care to avoid an economically unfeasible design.

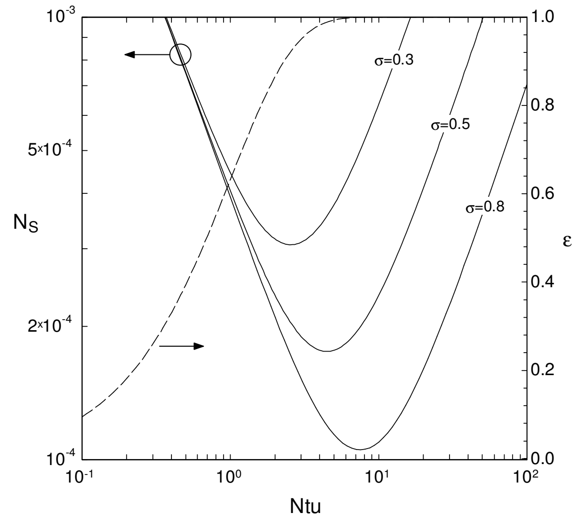

Figure 7: Effect of Ntu on N_S for various σ (Q=100 W, V=50 m^3/h, T_i=260K, A_f=0.02 m^2)

On one hand, since the coil temperature is treated as a floating parameter during the optimization exercise, the design for heat transfer enhancement leads to lower average temperature differences and, therefore, to a lower condensing temperature and a higher evaporating temperature. On the other hand, the optimization for pressure drop reduction yields a higher mass flow rate for the same pumping power, thus improving the heat transfer coefficient which also tends to reduce the condenser temperature or increase the evaporating temperature. Since the refrigeration system COP obeys the $T_e/(T_c–T_e)$ scale, it can be stated that the heat exchanger design that presents the best local (component-level) performance in terms of minimum entropy generation also leads to the best global (system-level) performance.

NOMENCLATURE

A_c	Minimum free flow passage	(m^2)
A_f	Face area	(m^2)
A_s	Heat transfer surface	(m^2)
c_p	Specific heat	(J/kgK)
D_h	Hydraulic diameter	(m)
D_t	Tube outer diameter	(m)
f	Friction factor	(-)
h	Heat transfer coefficient	(W/m^2K)
j	Colburn j-factor	(W/K)
k	Thermal conductivity	(W/mK)
L	Mass flow rate	(kg/s)
m	Thermal conductance	(W/K)
N_S	Entropy generation number	(-)
Ntu	Number of transfer units	(-)
p	Pressure	(Pa)
Pr	Prandtl number	(-)
Re	Reynolds number	(-)
Q	Heat transfer rate	(W)
s	Specific entropy	(J/kgK)
S_g	Entropy generation rate	(W/K)
T_c	Condensing temperature	(K)
T_e	Evaporating temperature	(W/K)
T_m	Mean flow temperature	(K)
T_s	Surface temperature	(K)
u_c	Maximum (core) velocity	(m/s)
u_f	Face velocity	(m/s)
V	Volumetric flow rate	(m^3/s)
W_p	Pumping power	(W)

Greek

ε	Heat exchanger effectiveness	(-)
ϕ	Finning factor	(-)
μ	Viscosity	(Pa s)
ρ	Density	(kg/m^3)
σ	Dimensionless free flow passage	(-)

REFERENCES

Barbosa JR, Melo C, Hermes CJL, Waltrich PJ, 2009, A Study of the Air-Side Heat Transfer and Pressure Drop Characteristics of Tube-Fin "No-Frost" Evaporators, *Applied Energy* 86, pp.1484-1491

Barbosa JR, Hermes CJL, 2008, Heat Transfer in Refrigeration Applications, *Heat Exchanger Design Handbook*, Chapter 3.26, Begell House, USA

Bejan A, 1996, Method of entropy generation minimization or modeling and optimization based on combined heat transfer and thermodynamics, *Rev. Gen. Therm.* 35, pp.637-646

Bejan A, 1987, The thermodynamic design of heat and mass transfer processes and devices, *Heat and Fluid Flow* 8 pp.258-276

Hermes CJL, 2012, Conflation of ε-Ntu and EGM design methods for heat exchangers with uniform wall temperature, *Int. J. Heat and Mass Transfer* 55, pp.3812-3817

Hermes CJL, Silva WL, Castro FAG, 2012, Thermal-hydraulic design of fan-supplied tube-fin condensers aimed at minimum entropy generation, *Applied Thermal Engineering* 36, pp. 307-313

Kakaç S, Liu H, 2002, *Heat Exchangers: Selection, Rating, and Thermal Design*, CRC Press, Boca Raton-FL, USA

Kays WM, London AL, 1984, *Compact Heat Exchangers*, McGraw-Hill, New York, USA

Kotcioglu I, Caliskan S, Cansiz A, Baskaya S, 2010, Second law analysis and heat transfer in a cross-flow heatexchanger with a new winglet-type vortex generator, *Energy* 35, pp. 3686-3695

Lerou PPPM, Veenstra TT, Burger JF, ter Brake HJM, Rogalla H, 2005, Optimization of counterflow heat exchanger geometry through minimization of entropy generation, *Cryogenics* 45, 659–669

Melo C, Silva LW, 2010, A perspective on energy savings in household refrigerators, *Sustainable Refrigeration and Heat Pump Technology Conference*, Stockholm, Sweden

Mishra M, Das PK, Sarangi S, 2009, Second law based optimisation of crossflow plate-fin heat exchanger design using genetic algorithm, *Applied Thermal Eng.* 29, pp. 2983–2989

Pussoli BF, Barbosa JR, Silva LW, Kaviani M, 2010, Air-side heat transfer and pressure drop characteristics of peripheral fin heat exchangers, *Int. Heat Transfer Conference*, Washington-DC, USA, IHTC14-23037

Saechan P, Wongwises S, 2008, Optimal configuration of cross flow plate finned tube condenser based on the second law of thermodynamics, *Int. J. Thermal Sciences* 47, pp. 1473-1481

San JY, Jan CL, 2000, Second-law analysis of a wet crossflow heat exchanger, *Energy* 25, pp. 939–955

Shah RK, Sekulic D, 2003, *Fundamentals of Heat Exchanger Design*, Wiley, New York, USA

ACKNOWLEDGMENTS

Financial support from the CAPES Agency (Grant No. AEX 8396-12-4), Government of Brazil, is duly acknowledged.